



Contents lists available at ScienceDirect

International Communications in Heat and Mass Transfer

journal homepage: www.elsevier.com/locate/ichmt

Thermal performances of Super Insulation Materials (SIMs): A comprehensive analysis of characteristics, heat transfer mechanisms, laboratory tests, and experimental comparisons

Ákos Lakatos^{a,*}, Elena Lucchi^b

^a University of Debrecen, Faculty of Engineering, Department of Building Services and Building Engineering, Debrecen 4028, Ótemető Str 2-4, Hungary

^b Politecnico di Milano, Department of Architecture, Built Environment and Construction Engineering (DABC), Via Bonardi 12, Milan 20133, Italy

ARTICLE INFO

Keywords:

Thermal conduction models
Super insulation material
SIMs
Aerogels
Vacuum insulation panels
Graphite EPS

ABSTRACT

New buildings are subject to more stringent regulations that focus on reducing inefficient energy consumption and eliminating associated harmful emissions. This challenge has been exacerbated by the current energy crisis. As a result, there has been an increase in the development of energy-efficient and environmentally friendly design strategies, technologies, and building materials. This study addresses critical knowledge gaps in Super Insulation Materials (SIMs), such as aerogel, vacuum insulation panels, and graphite-doped polystyrene foam. Despite their excellent insulation properties, these materials face challenges due to a lack of information on their properties, heat transfer mechanisms, test procedures for thermal evaluation, and performance comparisons between different types of SIMs. Through an innovative theoretical approach and laboratory tests, this study creates a complete scientific framework to understand thermal conduction models, performances, and characteristics in SIMs' application, compared to conventional insulations. We show thermal conductivity measurement results with excellent values belonging to vacuumized aerogels. We further state that graphite addition to white EPS reduces the thermal conductivity, but enhances the moisture up-take and infrared degradation.

1. Introduction

In recent decades, architecture has undergone significant transformations primarily driven by the increasing demand for energy and the recognition that fossil energy resources (e.g., petroleum, natural gas, coal) are depleting. Additionally, their prices have skyrocketed since the oil crisis of the 1970s, which has extended to the current global energy emergency. To address these challenges and achieve an appropriate indoor climate while minimizing energy consumption, it has become essential to incorporate a new building structure layer, such as thermal insulation that reduces the heat flow across the building envelope, minimizing overall heat losses or gains, and generating substantial energy savings in heating and/or cooling [1,2]. In an average uninsulated residential building, 30–40% of the total heat is lost through the external wall, 10–15% through the ground floor, 10% through the chimney, 20–25% through the roof, and 20–30% apply [2]. Effective thermal insulation is essential in reducing carbon dioxide (CO₂) emissions and promoting sustainability in the built environment. Proper insulation reduces the need for excessive heating or cooling, thereby lowering

energy consumption and associated carbon footprints. This decreases reliance on fossil fuels and contributes to global efforts for climate mitigation. Additionally, improved thermal insulation enhances indoor comfort, leading to healthier living environments and increased resilience to extreme temperatures [3]. Although various materials have been employed since ancient times using natural and local materials (e.g., notable vernacular examples include the use of animal hides for internal insulation of igloos and wood panels in mountain cabins) [3], their use has become more widespread in recent decades increasing the environmental impact of specific industries including the construction sector [4]. The development of these materials was closely related to the availability and affordability of recoverable energy sources in a specific territory. The production of most currently used insulation materials requires substantial reliance on hydrocarbons (or fossil energy) in their production processes, resulting in a significant carbon footprint. Currently, the environmental impact of specific industries is becoming increasingly problematic, and the construction sector is no exception [5]. A critical examination of their evolution in the building sector provides a deeper understanding of this concept. Since the mid-19th

* Corresponding author.

E-mail address: alakatos@eng.unideb.hu (Á. Lakatos).

<https://doi.org/10.1016/j.icheatmasstransfer.2024.107293>

Received 12 January 2024; Received in revised form 26 January 2024; Accepted 31 January 2024

Available online 6 February 2024

0735-1933/© 2024 The Authors. Published by Elsevier Ltd. This is an open access article under the CC BY-NC-ND license (<http://creativecommons.org/licenses/by-nc-nd/4.0/>).

century, materials of animal and plant origin (e.g., wood, hemp, cork, straw, bamboo, sheep's wool) have been replaced by various nature-related materials (e.g., brick filled with ash, wood fiber, expanded cork) with improved insulation capabilities. From the latter half of the 19th century through the early decades of the 20th century, numerous attempts were made to create artificial insulating materials. The advent of mass production of plastics in the mid-20th century introduced a new perspective for this industry with the production of expanded polystyrene (EPS), rigid polyurethane (PUR), polyisocyanurate (PIR) foams. Additionally, mineral materials (e.g., mineral wool, glass wool, rock wool) were introduced. However, many of these materials have not gained widespread recognition due to their short lifespan and unfavorable properties [6,7] (i.e., rock wool was introduced during this period but only gained widespread recognition many years later). The start of mass production of plastics in the middle of the 20th century brought a new perspective to the construction industry. Plastics and other artificially improved insulation materials became the most popular choices for insulation, leading to a decline in the use of natural materials. Their development accelerated in the 1970s due to external economic factors, such as the oil crisis, as people became widely aware of the finite nature of Earth's energy resources. Therefore, minimizing the utilization of energy sources became imperative. EPS foam, polyurethane foam (XPS), and mineral wool were the most frequently used materials due to their outstanding thermal capabilities and affordability. In recent years, the challenges posed by climate change have led to significant advancements in the field of thermal insulation. The increasing awareness of environmental impact has triggered a revolution in the insulation industry, resulting in the development of more sustainable and high-performance solutions. This shift in perspective has spurred research and development in advanced thermal insulation materials, with a focus on ecological and resilient concerns. In parallel to the building sector, thermal insulation materials have applications in various domains, including aeroplanes, automobiles, railways, and refrigerators. In some cases, their outer shell structure requires "thin" layers (e.g., 0.02–0.03 m). Technological advancements have led to the development of a more comprehensive range of thermal insulation. Nanostructured insulating materials were introduced to the market in the early-21st century as Super Insulation Materials (SIMs) with high thermal performance [8–18] achieved by reducing the thermal conductivity coefficient (λ or λ -value) [W/mK]. This value measures the ability of a solid material to transfer heat through a conduction. SIMs are increasingly used as internal thermal insulation due to their ability to lower insulation thickness by 30–50%, making them a viable alternative to conventional products. Although their remarkable insulating performance, they are expensive and lack sufficient information on their robustness, durability, long-term behaviour, and fundamental thermal qualities [19–29]. The literature shows the following shortcomings on SIMs:

- Clear analysis of the applicability of heat transmission principles.
- Assessment of the applicability of thermal performance analysis techniques.
- Performance comparisons among different SIMs.

Thus, the analysis of their performances, practices, and comparisons is necessary to close the knowledge and application gaps in SIMs research. The novelty of the study refers to the comprehensive overview of SIMs, which facilitates comprehension of their thermal, chemical, and physical properties for scientists, researchers, designers, developers, and practitioners. The identification and exploration of heat propagation models in SIMs compared to traditional insulation materials (white and graphite EPS) is a crucial advancement. This allows for a better understanding of the specific mechanisms of heat transmission in these materials, facilitating calculations, simulations, and measurements. Another innovative aspect is the analysis of both steady-state and transient test methods for measuring λ -value, defining their advantages and disadvantages in the context of SIMs. This critical examination

assists in selecting appropriate testing methodologies based on field experiences. Additionally, laboratory-based tests allow for the comparison of λ -values, sorption properties, and IR absorption tests of SIMs and common insulation materials, adding a practical dimension.

2. Materials and methods

The research aims to create a thorough scientific framework for SIMs by examining their features, theoretical underpinnings, and laboratory testing techniques to determine their thermal transmission properties. The research is structured into the following sections:

- Overview of SIMs, including materials' classification, characteristics, and production process (section 3).
- Heat conduction in solids with a detailed theoretical foundation on the thermal transmission models of aerogel and vacuum insulation panels (VIPs) (section 4).
- Laboratory testing methods for measuring the thermal performances of SIMs (section 5).
- Experimental comparison between the thermal performance of SIMs and conventional insulation materials by showing their applicability limits (section 6).

3. Brief overview of super insulating materials

SIMs do not have an official formal definition [29]. However, the International Energy Agency (IEA) - Energy in Buildings and Communities Programme (EBC) in Annex 65 started to work on this topic with numerous researchers and experts. According to that, SIMs use the Knudsen effect to suppress gaseous thermal conduction as a heat transfer mechanism. The following processes are realized to improve the thermal performance of an insulation material [30]:

- Heavy gases, such as argon and CO₂ with lower λ -value, are introduced into air-gaps and pores (e.g., foam or gas-filled materials).
- Pore size reduction in hollow spaces creates numerous collisions between gas and solid particles (e.g., nanoporous materials).
- Removing gas by evacuation, creating vacuum spaces within the material (e.g., vacuum materials).

According to these processes, SIMs are classified into the following categories [31]:

- Advanced Porous Materials (APM), divided into fumed silica and aerogel-based products.
- Vacuum Insulation Panels (VIPs).

3.1. Advanced porous materials

Advanced Porous Materials (APMs) have a nano-open porous structure with a porosity of approximately 97%, which outperforms conventional insulation materials that typically have a porosity range of 90–94% [32]. The solid structure consists of interconnected particles and pores, typically around 20 nm in size, with densities ranging from 50 to 250 kg/m³. APMs are classified into two main types [30]:

- The result of agglomerating hydrophobized pyrogenic amorphous silica dioxide particles into tertiary particles is fumed silica.
- Aerogel-based products are made using the sol-gel method with a precursor solution that usually consists of polymers or metal oxides.

Pyrogenic silica is a low bulk density, fine powder with a large surface area [32]. To produce silicon dioxide (SiO₂), silicon, hydrogen, and chlorine molecules are hydrolyzed in a high-temperature flame [33]. This results in small silica particles that oxidize. The particles fuse into a

fumed silica powder, useful in applications as an anti-caking and thickening agent. It can also control the viscosity of paints, varnishes, and silicone elastomers.

Aerogel-based products are manufactured using the sol-gel process [30]. This method involves the creation of a material in a liquid solution, which goes through a chemical process to turn into a gel and, finally, a solid [34]. The liquid colloidal suspension, also known as precursor or sol, gels forming a network of interconnected particles or polymers in three dimensions throughout the liquid. Specialized drying methods are used to remove the gel’s solvent, maintaining its porous nature and preventing collapse [35]. The resulting solid structure is called “aerogel”. Aerogel-based products are available in various forms, including monolithic, granular, fiber-reinforced, bonded, or packaged materials [31]. They can be also incorporated into different construction materials, such as composites, plaster, concrete, and panels [36]. The thermal performance of these materials is summarised below (Table 1).

3.2. Vacuum insulation panels

VIPs consist of an airtight multi-layer envelope that encloses a porous core, also known as filler material, from which air and gases have been removed [37]. The envelope is sealed under vacuum by a highly airtight and vapour-tight barrier, also known as a high barrier laminate. This vacuum eliminates gas conduction. The core material provides insulation and mechanical properties due to its open porous structure, which facilitates gas evacuation. The core is a board of pressed powder made from different insulation materials [38]. These materials can be categorized based on their pore size into:

- Sub-micrometer pores (up to 0.5 μm) include fumed and precipitated silica, silica aerogel in various forms (monolithic materials, blankets, or powders), and fine powders. They have a typical density of approximately 200 kg/m³ [32].
- Coarser pores (up to 100 μm) that contain organic open-celled foams (e.g., polyurethane, polystyrene, polyimide), mineral fibers (e.g., glass or rock fiber), inorganic granular materials (e.g., perlite, granular silica aerogel).

Adequate small pore size is advantageous to achieve and maintain the required vacuum level. Fumed silica, a fine white powder made of SiO₂, is frequently employed. The powder is compressed into boards, occasionally with added fibers for structural stability and infrared (IR) opacifiers to minimize IR radiative heat transfer. VIPs made of fumed silica have a central λ-value ranging from 0.004 to 0.0048 W/mK [32]. The declared λ-value ranges from 0.007 to 0.008 W/mK, considering thermal bridge effects and aging over 25 years. To reduce thermal bridge effects metallised high-barrier laminates are commonly used. These laminates consist of three layers of metallised (metal-coated) polymer films (PET) with an inner sealing layer of either polyethylene (LLDPE) or polypropylene (PP). Silica aerogel used in VIPs is produced through the sol-gel process, resulting in a material with pore sizes typically around

Table 1
General properties of different types of aerogel (Source: Author’s elaboration from [32]).

Properties	Granular silica aerogels	Silica aerogel composites	Organic aerogels	Synthetic amorphous silica boards
Density [kg/m ³]	50–250	50–250	50–250	50–250
λ-value [W/mK]	0.014–0.020	0.015–0.020	0.009–0.040	0.016–0.020
Water vapour permeability (μ) [–]	5–10	5–10	5–10	5–10
Hydrophobicity (contact angle) [°]	>160	140–160	140–160	140–160

20 μm and a mass density between 100 and 250 kg/m³. Its central λ-value is approximately 0.004 W/mK, while the declared value is 0.0135 W/mK [32]. Despite these advantageous thermal properties, the high cost of aerogel-core hinders their economic viability for large applications. VIPs with coarser pores have an average central λ-value of 0.002 W/mK, and a declared value between 0.035 and 0.040 W/mK [38]. The outer layer is made of aluminum foil for protection, and there is an inner sealing layer of either polyethylene or polypropylene. These laminates exhibit a non-negligible thermal bridge effect due to the significantly larger thickness of aluminum. To maintain the internal gas pressure at the required lower level, getters and desiccants are necessary. PUR and polystyrene (PS) foams are commonly used as core materials due to their open pore structure. However, their larger pore size requires a reduction of internal gas pressure by the same factor (normally <0.1 mbar) to have a negligible effect on the gas contribution to total heat transfer. Additionally, getters and desiccants are often used to reduce water vapour over time due to plastic releases. The central λ-value of VIPs ranges from 0.005 to 0.007 W/m K. These materials have a low density of around 50 kg/m³, making them suitable for weight-sensitive applications such as transport containers and boxes [32]. However, their unfavorable fire classification and stringent requirements on envelope tightness make them unsuitable for buildings. Mineral fiber cores have similar requirements for controlling internal gas pressure, with a lower average central λ-value of 0.0015 W/mK and higher thermal stability. However, the expected lifetime of 15 years remains a challenge for building applications.

4. Heat conduction

The λ-value is a crucial thermo-technical property of thermal insulation materials. Environmental factors, such as humidity and temperature fluctuations, moisture, freeze/thaw cycles, and ultraviolet (UV) radiation, can deteriorate their properties [39] (e.g., thermal performance of mineral fibers and natural-based fibrous insulation degrades due to water vapour [41], hydrophobization of APMs diminish due to environmental factors [32]). In addition, thickness variations and potential barrier layers can also influence this value [40]. This challenge is significant for SIMs. For instance, PUR foams filled with heavy gases and VIPs exhibit a gas exchange phenomenon over time, which increases the λ-value. This is due to incorrect envelope tightness or maintenance negligence [42]. Manufacturers aim to maintain a low λ-value after installation, considering the factors that may affect their long-term thermal performance [40]. Engineers need accurate λ-value and absorption capacity from laboratory tests to ensure effective planning. For this purpose, a brief introduction to heat conduction in solids and insulation materials (section 4.1) is fundamental.

The λ-value of homogeneous solids can be easily determined by measuring the equilibrium heat flow that flows in the sample as a result of the temperature gradient ΔT/Δx (K/m):

$$J_q = -\lambda(\Delta T/\Delta x) \tag{1}$$

where J_q (W/m²) is the thermal energy flow flux (the energy flowing through the unit cross-section during the unit time). The shape of eq. (1), which establishes the λ-value, implies that the distribution of thermal energy is a stochastic process. Instead of entering at one end of the sample and moving directly to the other, the energy diffuses through the sample while frequently colliding. The heat flux expression would only depend on the temperature difference ΔT (K) between the two ends of the sample (independent of sample length) if the energy flowed directly through the sample without deflection. The random nature of the conduction process requires the temperature gradient in the heat flux density expression [41].

The following expression for λ-value can be approximated by using the kinetic theory of gases:

$$\lambda = (1/3)(Cv) \tag{2}$$

where C is the volumetric heat capacity, v is the mean value of the velocities of particles, and l is the mean free path of particles between two collisions. Debye was the first to use these findings to explain λ -value in dielectric substances, using C as the phonons' heat capacity, average velocity, and l as their accessible mean route. We present the basic kinetic theory, which brings us to (2). The x-direction flux of particles is $(1/2)nv_x^2$. A flow of equal magnitude moves in the opposite direction, where n is the concentration of molecules in equilibrium. If c is a particle's heat capacity, it will lose energy $c \Delta T$ as it moves from a location with local temperature $T + \Delta T$ to a region with local temperature ΔT . The distance Δx between the ends of a particle's accessible route is now specified by:

$$\Delta T = (dT/dx)l_x = (dT/dx)v_x\tau \tag{3}$$

where τ is the average time between two collisions.

Therefore, the particle flux in both senses yields the following net energy flux:

$$J_q = -n < v_x^2 > c(dT/dx) = (1/3)n < v^2 > c\tau(dT/dx) \tag{4}$$

If v is a constant for phonons, the preceding equation can be written as:

$$J_q = (1/3)(Cvl)(dT/dx) \tag{5}$$

with $l = vl$, and $C = nc$, thus $\lambda = (1/3)(Cvl)$.

4.1. Heat conduction in insulation materials

The following model defines the overall, practical or total λ -value of inhomogeneous (cellular or fibrous) insulation materials. Downer we will summarize the heat propagation through different thermal insulations. Furthermore, for clarity purposes, we will present the transfer and forms of heat conduction through sketches (see Figs. 1 to 4). The heat spread in a cellular, fibrous, or porous (gas-filled) thermal insulation material is grouped into six terms: (i) λ -value through the solid skeleton ($\lambda_{c,s}$), (ii) λ -value through the gas particles ($\lambda_{c,g}$); (iii) λ -value through heat radiation (λ_r); (iv) λ -value through gas convection the terms (λ_{conv}) that have high importance in fibrous insulations; (v) λ -value through trapped air or air layer (λ_{pair}); and (vi) λ -value through holes (λ_{hole}) [27,38–44]:

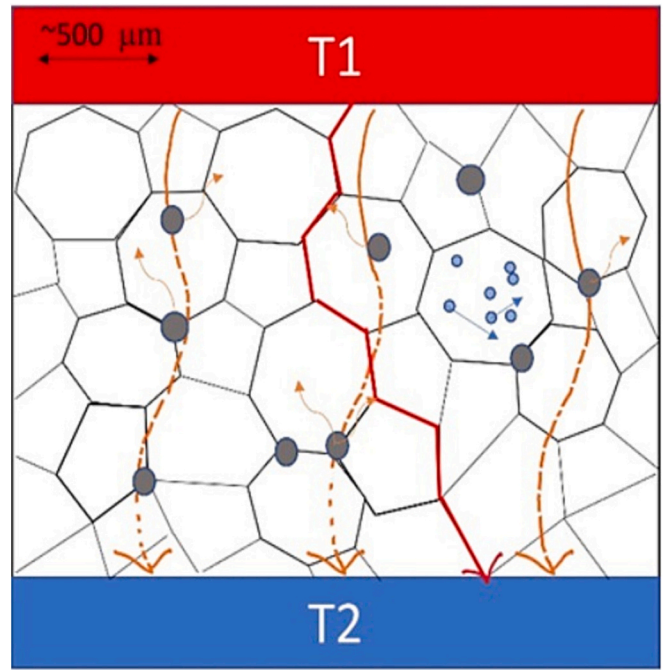


Fig. 2. Different forms of heat propagation in a graphite-doped cellular heat insulator [45].

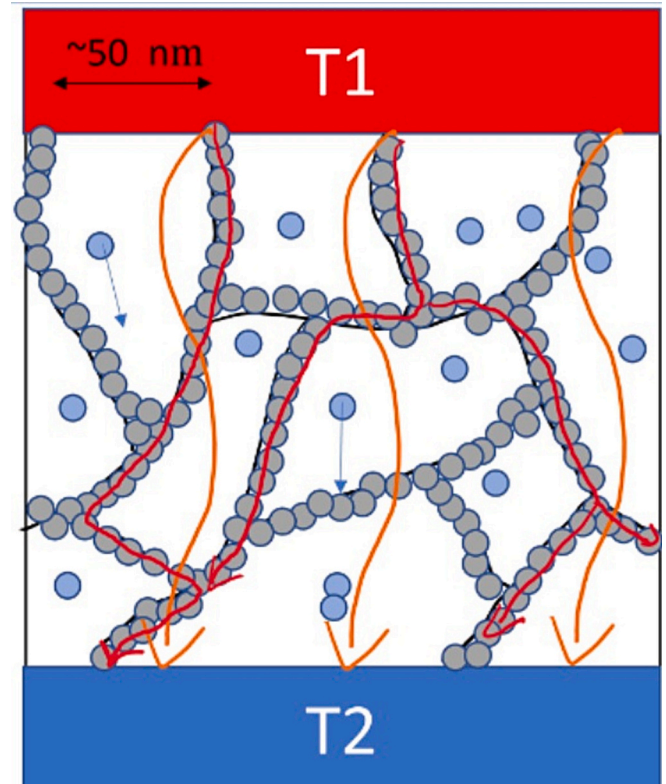


Fig. 3. Altered forms of heat transfer in aerogel (as advanced-porous material) [45].

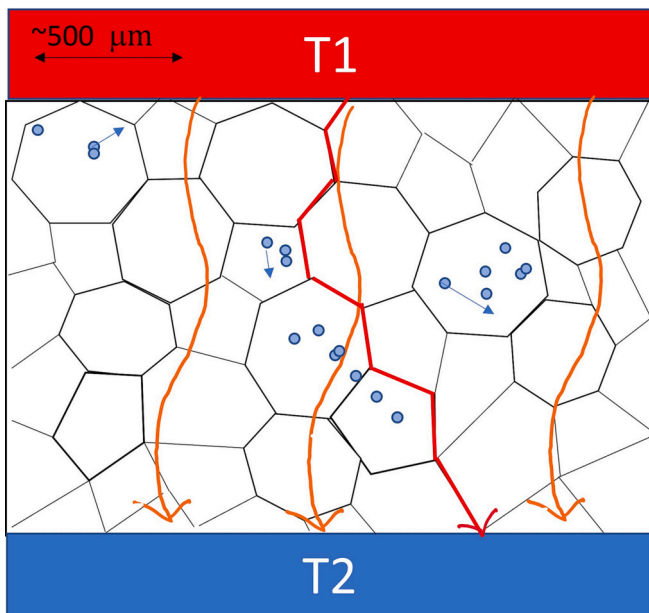


Fig. 1. Model of heat conduction mechanisms through a cellular/porous material, T1 and T2 represent the air temperature of the environment.

$$\lambda_t = \lambda_{c,s} + \lambda_{c,g} + \lambda_r + \lambda_{conv} + \lambda_{pair} + \lambda_{hole} \tag{6}$$

where (λ_t) is the total or effective heat conduction factor characteristic of the whole bulk material after measurements according to the rules of the ISO standards (8990, 8301 etc.). The last two terms describe

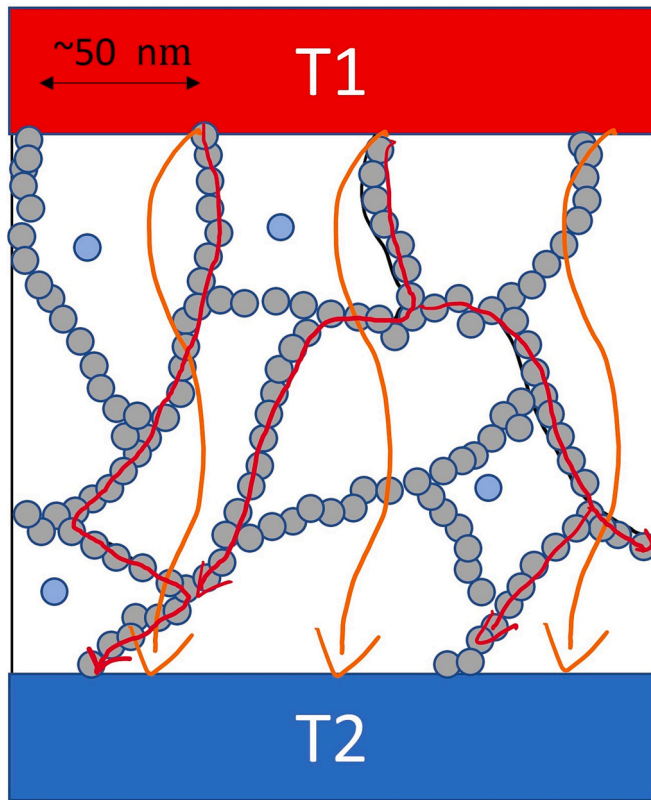


Fig. 4. Different forms of heat propagation in aerogel frame vacuum insulation

second-order processes (hole, pair) and occur due to the pressure difference. Usually, they can be neglected in these size ranges. Thus, λ_t is:

$$\lambda_t = \lambda_{c,s} + \lambda_{c,g} + \lambda_r + \lambda_{conv} \quad (7)$$

The following explanations can be introduced:

- ($\lambda_{c,s}$): The solid body's λ -value can be seen in heat transfer between atoms/molecules (lattice vibrations - phonons), chemical bonding among particles, and other processes (see red arrows in Fig. 1).
- ($\lambda_{c,g}$): The gas's heat conduction coefficient, which spreads from molecule to molecule as a result of the collision of gas constituents (see colliding blue dots in Fig. 1).
- (λ_r): The electromagnetic radiation emitted by the material's surface in the infrared range can be linked to the radiation component (see orange arrow in Fig. 1).
- (λ_{conv}): The term "conv(ection)" refers to the movement of air and moisture or the transportation of thermal substances. These values depend on temperature and pressure, particularly the gas-related thermal conductivity components. With increasing density (decreasing pore size) in the case of foamy materials, the convection term goes to zero and becomes negligible (see blue arrows in Fig. 1).

The high porosity of the material obstructs the propagation of phonons within the material, leading to a decrease in heat conduction through the solid framework as porosity increases. This phenomenon is visible in the aerogel's backbone. The elastic collisions between gas molecules determine the gas state. The thermal conduction ability of the gas phase is influenced by the average free path size of the molecules in the holes and the pore size, for aerogel to be an effective thermal insulator, its λ -value must be lower than that of free ambient air (0.025 W/mK) at 23 °C and 10^5 Pa pressure). This is achievable if the pore size is smaller than the typical free-path size of air molecules (~70 nm), preventing gas's thermal diffusion through the material. Pressure reduction can also achieve this. The Knudsen number, defined by eq. (9),

represents the ratio of the mean free path to the pore size (diameter). The pores' nanometric length reduces gaseous conductive and convective thermal transmission and radiation.

$$\lambda_{c,g} = \lambda_{g,0} / (1 + 2\beta Kn) = \lambda_{g,0} / (1 + (2^{1/2} \beta k_B T / \pi d_g^2 p \delta)) \quad (8)$$

$$Kn = \sigma_{mean} / \delta = k_B T / 2^{1/2} / \pi d_g^2 p \delta \quad (9)$$

where,

$\lambda_{g,0}$: the standard state thermal conductivity coefficient of the gas; β : the collision of molecule-wall interaction (<2); k_B : the Boltzmann constant (J/K); P is the pressure (Pa); d : collision diameter of the gas molecule (nm); δ : the representative pore size (nm); σ_{mean} : the average free path of the gas particles (nm).

In this instance, the gas molecules contained within the pore clash with the pore wall rather than one another. The Knudsen number is less than one if the average free route length of the molecules is less than the cell dimension and more than one otherwise. Heat moves randomly across nearby oscillators in materials like aerogel that have pores between 10 and 100 nm in diameter.

The radiation part of heat conduction can be defined based on eq. (10):

$$\lambda_r = 16 n_r^2 T^3 / 3 \alpha_R \quad (10)$$

where. n_r : ractive index; σ : a Steffan-Boltzmann constant (5.67×10^{-8} W/(m²K⁴)); α_R : Rosseland average absorption coefficient. The extinction coefficient and refractive index are significant factors that define the scope of a material's radiative qualities.

At a given temperature, increasing the energy (heat) absorbing ability of materials (by adding absorbance and reflective nano-micro particles) is an efficient method to reduce the radiative part of heat conduction λ_r , a way for this the addition of graphite/carbon particles to expanded polystyrene (Fig. 2) [45–49].

The downer formula (Eq. 11).

$$\lambda_s = \lambda_0 (\rho_s \nu_s / \rho_0 \nu_0) \quad (11)$$

where ρ_s is the density of the porous material, ρ_0 is the density of the material without pores, λ_0 is the heat conduction factor of a completely "dense" solid body, ν_s is the sound propagation speed in the material, and ν_0 is the sound propagation speed in the non-porous material. Aerogel's high degree of porosity causes a decrease in density and a slower rate of sound transmission.

More simply put, the density of the aerogel alone determines the solid phase thermal conductivity of SiO₂ aerogel, which is expressed as follows in the function of density, where K is constant:

$$\lambda_s = K \rho^{3/2} \quad (12)$$

Furthermore, Eq. 12 can be further simplified with (α) percolation exponent:

$$\lambda_s = \lambda_0 (\rho_s / \rho_0)^\alpha \quad (13)$$

The aerogel's high degree of porosity causes a decrease in density and a slowing down of propagation (Fig. 3) [45,50–52].

Vacuum panels achieve low λ -value because they do not contain air or gas. VIPs manufacturing process is based on several simple steps. As a first step, the core material is pressed into a specific mold, with the help of which all the air is forced out of the material. VIPs' boards are generally made in a maximum size of 60 × 100 cm, but this size can vary according to demand. Then, a vacuum pump is used to further evacuate the gas in the core material (note that there is no perfect vacuum inside the materials) [53–59]. The sensitive point of vacuum panels is the sealing. Its heat conduction factor is thus practically divided into two components, radiation and conduction through the frame of the solid core material (Fig. 4), see Eq. 14:

$$\lambda_t = \lambda_{c,s} + \lambda_r \quad (14)$$

5. Thermal conductivity measurements

Thermal conductivity measurements are traditionally divided into:

- Direct thermal conductivity measurements (section 5.1).
- Indirect thermal conductivity measurements (section 5.2).

Their application to SIMs is evaluated (section 5.3).

5.1. Direct thermal conductivity measurements

Standard laboratory tests for measuring λ -value in insulating materials are divided into steady-state and transient methods [55]. Steady-state methods measure the thermal performance under equilibrium conditions, where temperatures remain constant and stationary throughout the testing period at each point of the sample [56]. The λ -value of homogeneous, plane, parallel, and uniform materials results in one-dimensional (1-D) heat flux [57]. Therefore, the Fourier's Law is employed to simplify the calculation [55]. Standard methodologies include:

- Guarded Hot Plate (GHP) method.
- Heat Flux Meter (HFM) measurement.

The GHP apparatus is composed of: (i) two metal plates to measure J_q ; (ii) several temperature sensors to measure the ΔT ; (iii) a heat source (typically a water circulation system) to generate uniform and controlled temperature conditions; (iv) an insulating guard that surrounds the heated plate to minimize heat loss [55]. The sample is placed between the two plates, and one is electrically heated at a controlled temperature (T). The temperature of the guard is maintained at the same temperature as the heating plate. In this way, a ΔT is created across the sample. When the steady state condition is established, the heat flow rate (Φ [W]) = power generated by the hot plate) is directly proportional to the electrical power supplied to the heating plate [58]. Thus, it is calculated from the measured voltage U [V] and the electric current induced I [A] as $\Phi = U \times I$. The λ -value is calculated from the heat input (Φ), ΔT , and dimensions of the sample in terms of area (A) [m²] and thickness Δx [m].

$$\lambda = \Phi \Delta x / \Delta T A \quad (15)$$

The test procedure is defined by the standards ISO 8301:1991 [60], EN 1946-2:2001 [61], EN 12667:2001 [62], EN 12664:2001 [63], ASTM C177:2010 [64], ASTM C1043:2019 [65], and ASTM C1044:2020 [66].

HFM assesses the overall heat transfer through a specimen, excluding contributions from solid and gas phase thermal conduction, radiation, and convection. This method determines the λ -value and thermal resistance (R or R-value) [m²k/W] [55] of a material. This apparatus is composed of: (i) one or two heat flux transducers to measure J_q ; (ii) a heating unit; (iii) a cooling unit; and (iv) thermistors or thermocouples to measure the ΔT and control the temperature. The thermocouples and heat flux transducers are commonly embedded within the apparatus but can also serve as external devices. The sample is positioned between the heating and cooling units, directly in contact with the transducer(s). The temperature of these units is regulated by Peltier elements that generate a voltage due to the ΔT in a metal. This voltage utilizes the Seebeck effect to convert thermal energy into electrical energy. A linear dependency between Φ and measuring signal is assumed. The Φ through the sample is measured when the temperature gradient is applied using Eq. 15. To reduce non-linearity errors between Φ and the measuring signal and establish their precise relationship, calibration measurements must be repeated using a reference sample with a known λ -value value similar to the one under consideration. The test procedure is defined by the standards ISO 8302:1991 [67], EN 1946-3:1999 [68], EN

12667:2001 [62], EN 12664:2002 [63], ASTM C518:2010 [69], and ASTM C1363:2019 [70].

Transient methods measure the thermal properties during the heating process by analyzing its response signal to a pulse required to increase its temperature. These methods typically require a short duration (a few minutes) compared to steady-state tests, which may take several hours [55]. Needle probes usually carry out transient methods, as follows:

- Transient Hot Wire (THW) method.
- Transient Plane Source (TPS) method.
- Laser Flash method or Laser Flash Analyser (LFA).

THW measures the λ -value of materials in a wide temperature and pressure range. The apparatus consists of a thin metal wire with infinite length, sandwiched between two identical samples. It is immersed in a fluid and serves simultaneously as an electrical heat source and resistance thermometer. The measurement relies on recording the transient temperature rise caused by a step voltage, generally in 120 s [55]. As the power remains constant, voltage fluctuations correspond to an alteration in the sensor's resistance. The λ -value is automatically calculated from Eq. 15 considering the slope of the linear temperature profile over time ($\Delta T / \Delta t$). Due to the concise duration, the measurement is highly accurate, thanks to the absence of thermal convection and the lack of need for calibration. The procedure is described by standards ISO 8894-1:2010 [71], EN 993-15:2005 [72], and ASTM C:1113:2013 [73].

TPS measures a material's λ -value and thermal diffusivity (α) [mm²/s] by analyzing its response to a thermal pulse that elevates its temperature [55]. The apparatus comprises a flat-shaped sensor with a circular double metal spiral, typically made of electrically conducting nickel. This sensor is sandwiched between two protective layers of thin polyimide, commonly made of Kapton, or Mica, which provides electrical insulation and mechanical stability to the sensor. The sensor is positioned between two identical samples and functions as both a heat source and a resistance thermometer. It is continuously heated during the test, and changes in voltage are recorded. Voltage fluctuations correspond to alterations in the resistance of the spiral as the power remains constant. The heat produced is dissipated into the sample on both sides of the sensor, influenced by the thermal transport properties of the material. These properties are calculated using a mathematical model that analyses the temperature variation related to the time response of the sensor. The procedure is defined by the standard ISO 22007-2:2015.

LFA measures the thermal diffusivity (α , m²/s) of a material. It is based on the temperature rise of one side of a sample subject to a short laser pulse (15 J) from the other side. The surface temperature is propagated as a heat wave through the material, and it is detected on the opposite side by an infrared measuring device. The speed of temperature propagation depends on the α of the material, which is directly associated with the λ -value, density (ρ), and specific heat capacity (cp):

$$\lambda = \alpha \rho c_p \quad (16)$$

The procedure is defined by the standard ASTM E1461-01:2013 [74].

Other non-standard tests are illustrated in the literature, but their practical application and reliability have not been empirically examined or widely tested in SIMs applications. Pros and cons of each standard procedure are detailed below according to the literature review and practical experience in our laboratories (During the measurement at least 25 °C temperature difference should be kept and both the wall and air temperatures must be registered at the "cold" and also at the "warm" side. At the same time, the supplied heat and/or the heat flux through the wall must be also registered.

5.2. Evaluation of the applicability to SIMs

Pros and cons of the application of these thermal conductivity measurements to SIMs are evaluated before (Table 2). Table 2).

5.3. Indirect methods

Two other test procedures are presented in the EN standard, ISO 8990 [75]: the calibrated chamber method and the guarded hot box method. They can be supposed as an indirect method for the measurement of thermal conductivities of insulation materials, as a basis of a wall structure. These methods are also steady-state methods, but these can be called indirect methods due to the following reasons: through the measurement, the thermal transmission of walls and wall structures can be characterized, and from the thermal resistances the thermal conductivities can be calculated. The space requirement of the method is significantly larger than that of the methods mentioned in the point above, and the length of the test procedure is much longer. Both tests require two adiabatic chambers with about 3–4 m² base area, with a dividing wall built from a masonry wall. At first, the thermal resistance (R₀, m²K/W) of the base wall must be measured without insulation, then

Table 2
Pros and cons of different techniques for λ-value measurements in SIMs.

Test	Pros	Cons
GHP	Guarded heat flow, absolute measurement method, high-temperature range	One specimen and two specimen method, long measurement time
HFM	Individual samples measurement, steady-state method, <2% accuracy, size, acceptable measurement time. Suitable for thermal insulation materials	Low to medium conductivity (only insulation materials), relative measurement method
THW	Short measurement time Direct determination of λ-value No calibration required Adequate measurement accuracy (e.g., ±10% for aerogels) Suitable for thin materials	Requires two identical samples in size, structure, and density Significant increase of the radiative thermal conductivity with high temperatures Embrittlement risks (e.g., pure aerogel, VIPs)
TPS	Short measurement time Reduced effects of the finite size and temperature distribution Adequate for isotropic materials	Need to reduce the resistance between the sensor and the sample Significant increase of the radiative thermal conductivity with high temperatures Not applicable to anisotropic materials (e.g., VIPs) Not applicable to low strength and poor toughness materials (e.g., pure aerogel) Embrittlement risks (e.g., pure aerogel, VIPs)
LFA	Short measurement time A robust and reliable method for determining the α-value of materials	λ-value is derived from α-value Adiabatic measurement cannot be conducted Radial losses within the sample Facial losses into the sample holder Low accuracy of measurement on porous and semi-transparent materials (e.g., aerogels)
Calibrated chamber	Measurement of wall structures Almost real circumstances can be fixed	Long measurement time (2–3 days) Space requirements, thermal bridges can be formed
Guarded hot box	Measurement of wall structures Almost real circumstances can be fixed Less thermal bridges than calibrated chamber	long measurement time (2–3 days) Space requirements

the thermal resistance of the wall with insulation should be defined (R, with a thickness of d [m].) By using eq. 17 the thermal conductivity can be found.

$$\lambda = d / (R - R_0) \tag{17}$$

During the measurement at least 25 °C temperature difference should be kept and both the wall and air temperatures must be registered at the “cold” and also at the “warm” side. At the same time, the supplied heat and/or the heat flux through the wall must be also registered.

5.4. Evaluation of the applicability to SIMs

Pros and cons of the application of these thermal conductivity measurements to SIMs are evaluated before (Table 2).

6. Experimental comparison between the thermal performance of insulation materials

We executed laboratory tests to see the applicability limit of the above-mentioned thermal insulation materials [6]. Changes in the environment, such as solar irradiation, moisture, and temperature change, can affect the thermal performance of the insulation materials. In some cases, during the refurbishment or building construction, the rapidly changing weather can modify the thermal parameters of the building materials. We executed a comparative laboratory test row to simulate the environmental effects, including thermal conductivity, sorption, and infrared absorption measurements. The test conducted refers to λ-value (section 6.1.1), sorption (section 6.1.2), and absorption (6.1.3) measurements.

Four different insulation materials were tested:

- White conventional pure EPS.
- Graphite EPS.
- Pyrogel aerogel.
- Homemade pyrogel aerogel-based vacuum insulation panel.

Four samples with 0.20 m × 0.20 m and 0.05 m thickness from the EPS and graphite EPS were used for the λ-value measurements, while the aerogel and the aerogel VIP had about 0.01 m thickness with a base area of 0.17 m × 0.17 m. The white EPS and the graphite EPS had about 15 kg/m³ density, while the pyrogel aerogel had 216 kg/m³ density. Moreover, the pyrogel aerogel was used as the core material of the pilot vacuum insulation panel. It was placed in the thin plastic bag, and with a vacuum-packer, a part of the air was removed, and the edges were closed with heat. This material was created to see the reduced λ-value. Four samples with a 0.10 m × 0.10 m base area with the thickness mentioned above were used for the sorption measurements. Moreover, samples with these geometries were used for the IR absorption tests. The materials’ features (Fig. 5) and key declared properties (Table 3) have been collected and shown. White as well as graphite EPS is not part of the superinsulation materials, but for comparison we also tested them. Still, during the manufacturing of these materials, nano- or micro-sized graphite and carbon flakes are added to the polystyrene melt, increasing the thermal insulation capability. It is said that carbon contaminants added to insulation materials can decrease the material’s thermal conductivity.

Below are described the tests conducted (section 6.1) and the thermal performances achieved (section 6.2) for these materials.

6.1. Thermal performance measurements

On these materials have been made the following measurements:

- Thermal conductivity measurements (section 6.1.1).
- Sorption measurements (section 6.1.2).

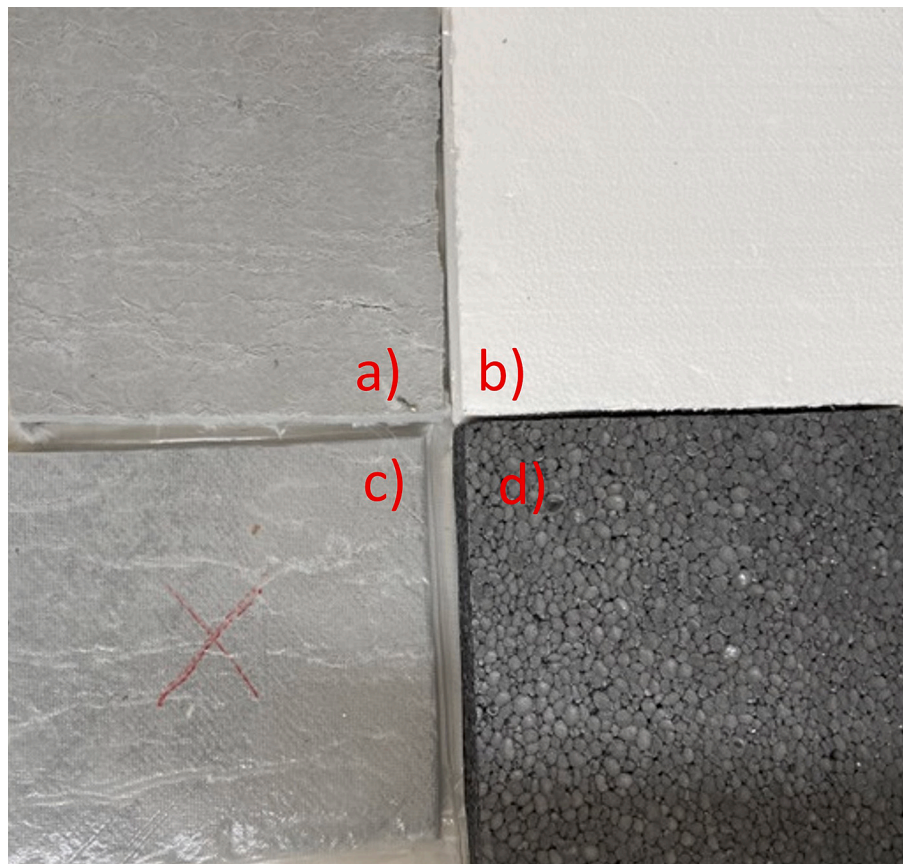


Fig. 5. The tested materials: a) Pyrogel aerogel, b) white EPS, c) vacuumized pyrogel aerogel, d) graphite EPS.

Table 3

The declared properties of the tested materials (Source: Author’s elaboration).

Material property	White EPS	Pyrogel	Graphite EPS
Declared Thermal conductivity [W/mK]	0.034	0.02	0.032
Density [kg/m ³]	16	190	15
Fire category	E	A2-s1, d0	E
Contaminants	H, C	Fe, Ca, S O, Mg, Al, Si, Ti,	C, H

- IR absorption test (section 6.1.3).

6.1.1. Thermal conductivity measurements

The thermal conductivity mentioned above is a crucial thermal parameter of buildings, especially thermal insulation materials. This value and the importance of it was identified above. The λ -value of the materials with 0.20 m × 0.20 m base area were examined by applying a Netzsch Heat Flow Metre 446 S. The measurements were executed according to ISO 8301 [60]. Four materials were separately analyzed, and the final values were the mean of each measurement row. The instrument is standardised, and the precision of the test results is <2%. The device is supplied with a cooler made by Julabo to achieve thermal steadiness quickly and reliably [11; 47].

6.1.2. Sorption measurements

The moisture sorption behaviour of building materials is a crucial concept. The equilibrium moisture versus relative humidity curves at a specific temperature graphically predict the water up-taking capability. It can also be applied as the water activity versus moisture content

curve. The absorption isotherm’s form can change depending on the particular insulation material. The features of moisture absorption can be influenced by pore sizes, surface qualities, and material compositions that differ. The insulation material’s durability, structural integrity, and thermal performance can all be adversely impacted by excessive moisture absorption. Therefore, producers and users of thermal insulation materials consider moisture absorption behaviour to choose the right products for specific applications and guarantee long-term performance.

The sample’s sorption isotherms were measured using a milligram precision balance in conjunction with the VentiCell drying apparatus and the ClimaCell climate chamber. Four representatives from each with a base area of 10 cm × 10 cm were used for the measurements, and the concluding results were the mathematical average of the four measurements. The trials were conducted at 23 °C with a range of relative humidity levels (30, 50, 65, 80, and 90%), following the guidelines stated in EN ISO 12571. Sorption isotherms reveal the samples’s surface microstructure and wetting characteristics [44].

6.1.3. IR absorption test

Solar, especially infrared irradiation, can harm building materials. Depending on the properties and content of the material, infrared (IR) radiation can have a variety of impacts. The following are some typical outcomes noted:

- Thermal heating: Infrared radiation interacts with materials to produce heat. The temperature, phase transitions, and molecular vibrations of the material can all be impacted by the heat produced.
- Surface modification: Infrared radiation can cause surface alteration in certain materials. IR radiation, for example, can enhance material density or cross-linking in polymers, improving mechanical properties and boosting resistance to chemical deterioration.

- Chemical excitation: Radiation at specific infrared wavelengths can directly stimulate particular chemical bonds within a substance. This excitation can have many effects, including changes in the material’s properties, chemical reactions, and molecular structures.
- Temperature-dependent reactions: High-intensity infrared radiation can significantly elevate a material’s temperature, allowing for temperature-dependent reactions. Depending on the substance and precise temperature range reached, these processes may involve sintering, pyrolysis, or breakdown.
- Absorption and reflection: Various materials show different absorption and reflection characteristics in the infrared spectrum. While certain materials reflect a substantial portion of the infrared radiation received, others efficiently absorb infrared light and produce more thermal energy.
- Contactless heating: The ability to heat materials without coming into contact with them makes infrared radiation crucial for many industrial processes. Noteworthy, the effects of infrared radiation can vary significantly depending on the specific wavelength, intensity, length of exposure, and characteristics of the material subjected to the radiation. Following Pan et al.’s recommendations, we used a 100 W Philips short-wave IR lamp to analyze the sample’s infrared absorption [47,76–80]. The graphite EPS samples and pure white polystyrene samples from the same manufacturer were positioned under the lamp at a set distance and had the same compressive strength (80 kPa). The measurement order was based on the one Pan and his associates described in Ref. [77]. A IR thermocamera of the Testo 883 design was also used to experiment further. One by one, the samples were exposed to light from the lamp alone, and as they heated, the surface temperature was measured.

6.2. The comparison of thermal performances

λ -value (section 6.2.1), sorption (section 6.2.2), and IR-absorption (6.2.3) performances of these materials have been compared.

6.2.1. Thermal conductivities comparison

Thermal conductivity is a key thermal property of thermal insulation materials. The lower the thermal conductivity, the better the thermal insulation capacity of the material. Thermal conductivity measurements were executed to compare the thermal insulation capability of the materials. In Fig. 6, one can see the decrease of the λ -value of the different materials. The thermal conductivities were measured at 10 °C mean temperature with 20 °C temperature difference with Netzsch HFM. Firstly, one can see about a 15% difference in the thermal conductivities

between pure (white EPS) and graphite EPS. The reason for this was mentioned above. At a given temperature, increasing the energy (heat) absorbing ability of materials (by adding absorbance and reflective nano-micro particles) is an efficient method to reduce the radiative part of heat conduction. Furthermore, the pyrogel aerogel has 65% less thermal conductivity than the white EPS, while the pyrogel-based VIP (vacuumized) has 18% lower thermal conductivity than the pyrogel (Fig. 6).

Following the analysis of the results presented in Fig. 6, we can state the excellent thermal conductivity of aerogels compared to the polystyrene derivatives. The thermal conductivity of the pyrogel aerogel is about half of the white EPS, while after eliminating the gas from the fibers of the pyrogel aerogel a further 20% reduction in the thermal conductivity can be found.

6.2.2. Sorption isotherms comparison

Sorption isotherms of each material (excluding pyrogel VIP) were registered (Fig. 7) in a climatic chamber after drying them. One can see that the highest values belong to the aerogel, due to its fibrous nature, while graphite EPS takes more water than white EPS. The containing carbon particles can explain it. Carbon particles are exquisite getter materials with a particular surface area, having a place for moisture take-up. Pyrogel is a fibrous aerogel with a strong adhesion relationship between the material and water vapour in the ambient air. The moisture uptake of the PS derivatives has a maximal moisture content of <2%.

6.2.3. Infrared absorption test

Each insulation sample was irradiated with an IR lamp, and the surface temperature was registered with a thermocouple (Testo 905) in the function of the elapsed time during the irradiation (see Fig. 8 a)). Infrared irradiation measurement is a tool to analyze the interaction of the energy wave with the substance through reflection, absorption and emission [79]. One can see in Fig. 8 b) that the measured surface temperature of the graphite EPS is two times greater than the surface temperature of the other two materials after IR irradiation. Moreover, due to the energy absorption, the graphite EPS samples are damaged through melting, the state of the graphite EPS sample before irradiation can be seen in Fig. 8 c) while the state of the sample after irradiation is presented in Figure b). The reason for this can be found in the graphite EPS. Once carbon particles have a dark colour, graphite particles can absorb a significant amount of heat energy. This process causes a temperature rise in the material itself, and after reaching the melting point of the graphite EPS, the material is damaged, and the material’s structure changes through contraction and shrinkage. White EPS and pyrogel

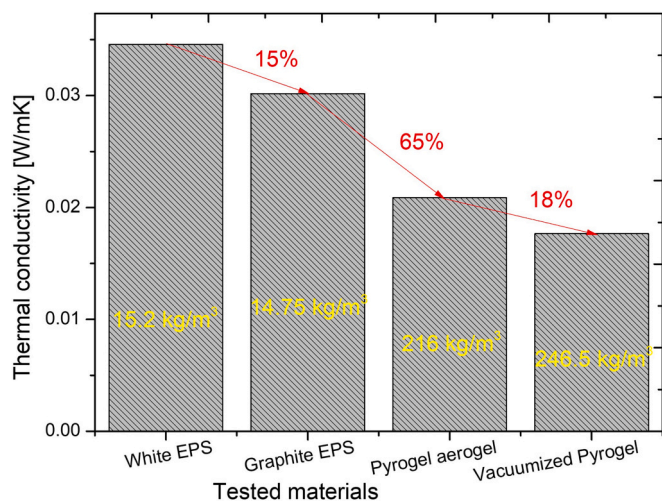


Fig. 6. The comparison of the measured thermal conductivities of different insulation materials.

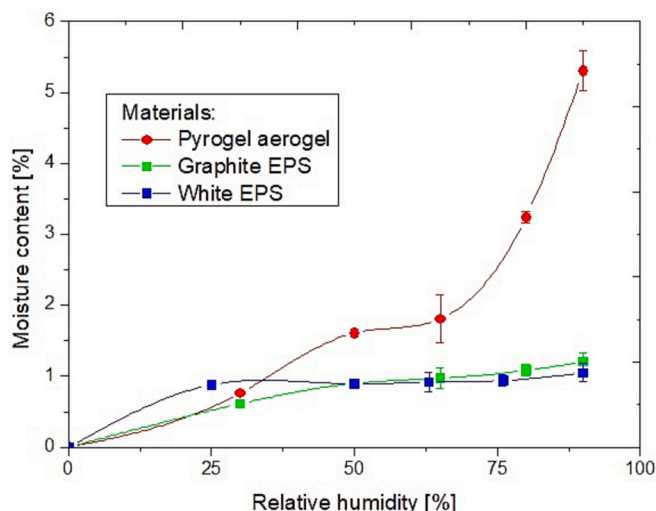


Fig. 7. The comparison of sorption isotherms of different insulation materials

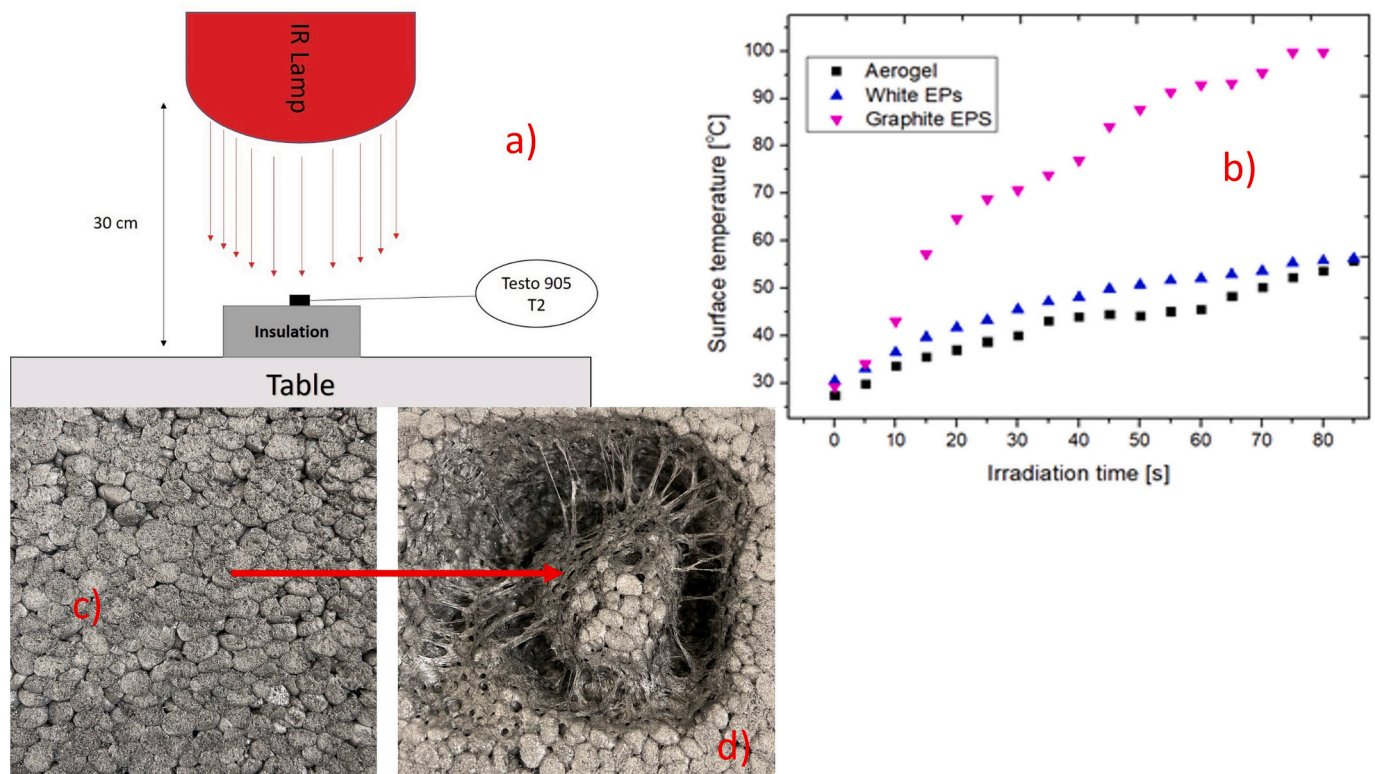


Fig. 8. (a) The measurement order of IR absorption test; b) surface temperature change during irradiation of different insulation materials, c) graphite EPS before irradiation; d) damaged graphite EPS after irradiation

materials do not suffer any structural-physical changes.

6.2.4. Applicability limit of the tested materials

We collected the applicability limits of the insulations in tabular form based on the laboratory measurements. These are represented in Table 4.

Table 4
The applicability of the tested materials.

Environment	White EPS	Gray EPS	The tested aerogel	Homemade VIP
Humid	Yes	Yes	Yes-but should be protected from moisture load	Yes
Intense solar irradiation	Yes	Yes-but should be protected from direct solar load	Yes	Yes
Little or medium sized available space (thickness 1–5 cm)	No	No	Yes	Yes
Large surface area	Yes	Yes	In exceptional cases: e.g.: historical/heritage buildings or similar.	
Dwelling house	Yes	Yes	Yes: As additional/extra insulation or where space needs to be saved	Yes: As additional/extra insulation or where space needs to be saved

7. Conclusions

Thermal insulation is crucial for optimising energy consumption and addressing climate-related issues. This aspect concerns many applications in various sectors, from buildings to transportation, automotive to industrial plants. Here, accurate knowledge of the thermal parameters of insulation materials is essential for designing these objects. Nominal values provided by manufacturers often depend on specific measurement conditions and instruments. After presenting a brief history of the innovation of insulation materials in the building sector (section 1), the study presents an extensive overview of the characteristics and production processes of superinsulation materials (SIMs), such as aerogel and vacuum insulation panels (VIPs) (section 3). Additionally, heat propagation models (section 4) and laboratory tests for measuring thermal conductivity (λ -value) applicable to these materials have been explained (section 5). Finally, λ -values, sorption properties, and IR absorption tests of common insulation materials and SIMs were compared using laboratory-based tests. A homemade pilot vacuum insulation panel, was also presented to show the vacuum’s effect on the thermal conductivity.

The point-to-point findings are as follows:

- After the thermal conductivity measurements, we deduced that the graphite/carbon flakes reduce the expanded polystyrene’s thermal conductivity by at least 15%. Suppose one eliminates the filling gas (air) from the fibers of the fiber-reinforced aerogel samples. In that case, its thermal conductivity decreases by about 20%, while without vacuumization, it has 65% less thermal conductivity than conventional white EPS.
- Sorption measurement shows that the fibrous aerogels take up much more moisture from the environment than the EPS, while the graphite flakes result in a higher equilibrium moisture content than white EPS.

- IR absorption measurement results show structural degradation of graphite EPS.

The novelty of the study lies in the following aspects:

- Creation of an overview of SIMs that allows for easy reading of their thermal, chemical, and physical properties.
- Identification of heat propagation models in SIMs, focusing on processes and mechanisms that differ from other insulating materials.
- Analysis of the tests for measuring λ -value in steady state and transient methods, defining the advantages and disadvantages of each technique about SIMs.
- Laboratory-based comparison of the tested insulation materials.

CRedit authorship contribution statement

Ákos Lakatos: Writing – review & editing, Writing – original draft, Visualization, Validation, Supervision, Software, Resources, Project administration, Methodology, Investigation, Funding acquisition, Formal analysis, Data curation, Conceptualization. **Elena Lucchi:** Writing – review & editing, Writing – original draft, Supervision, Methodology, Investigation, Conceptualization.

Declaration of competing interest

The authors declare that they have no known competing financial interests/personal relationships that could have appeared to influence the work reported in this paper.

Data availability

Data will be made available on request.

Acknowledgements

Project no. TKP2021-NKTA-34 has been implemented with the support provided by the Ministry of Innovation and Technology of Hungary from the National Research, Development and Innovation Fund, financed under the TKP2021-NKTA funding scheme.

References

[1] R. Daneshzarian, U. Berardi, Nano-enhanced thermal energy storage coupled to a hybrid renewable system for a high-rise zero emission building, *Energy Convers. Manag.* 291 (2023) art. no. 117301.

[2] S. Hámori, F. Kalmár, Hydraulic balancing analysis of a central heating system with constant supply temperature, *Environ. Eng. Manag. J.* 13 (11) (2014) 2789–2795.

[3] B. Tejedor, E. Lucchi, I. Nardi, Application of qualitative and quantitative infrared thermography at urban level: Potential and limitations, in: D. Bienvenido-Huertas, J. Moyano-Campos (Eds.), *New Technologies in Building and Construction*, Lecture Notes in Civil Engineering, vol. 258, Springer, Singapore, 2022, https://doi.org/10.1007/978-981-19-1894-0_1.

[4] Lucchi E. Schito, Advances in the optimization of energy use in buildings, *Sustainability* 15 (2023) 13541.

[5] P. Santos, E. Lucchi, S. Carlucci, Editorial: global excellence in sustainable design and construction: Europe 2023, *Front. Built Environ.* 9 (2023) 1335915.

[6] X. Xu, S. Yu, H. Sheng, Q. Li, S. Ni, Feasibility analysis of nearly zero-energy building design oriented to the optimization of thermal performance parameters, *Buildings*. 13 (10) (2023) 2478, <https://doi.org/10.3390/buildings13102478>.

[7] Song He, Xiyu Wu, Xiaoqian Zhang, Junwei Sun, Fuliang Tian, Saiping Guo, Du Haipeng, Ping Li, Yajun Huang, Preparation and properties of thermal insulation coating based on silica aerogel, *Energy Build.* 298 (2023) 113556 (ISSN 0378-7788).

[8] U. Heineman, nnext 65 Long-Term Performance of Super-Insulating-Materials in Building Components and 586 Systems. Report of Subtask I: State of the Art and Case Studies, EBC Annex 65, 2020.

[9] J. Wernery, F. Mancebo, W.J. Malfait, M. O'Connor, Jelle B. Petter, The economics of thermal superinsulation in buildings, *Energy Build.* 253 (2021) 111506.

[10] Yu Feng, Yanzhong Li, Yin Hai Zhu, Numerical and experimental investigation on the thermal insulation performance of low temperature cold box, *Int. Commun. Heat Mass Transf.* 36 (9) (2009) 908–991.

[11] A. Lakatos, A. Csík, I. Csarnovics, Experimental verification of thermal properties of the aerogel blanket, *Case Stud. Thermal Eng.* 25 (2021) 100966.

[12] A.K.I.N. Süleyman Kamil, Mustafa Alptekin, Examining the performance of thermal insulation materials used in buildings for noise insulation, *Case Stud. Thermal Eng.* 51 (2023) 103556 (ISSN 2214-157X).

[13] A. Lamy-Mendes, A.D.R. Pontinha, P. Alves, P. Santos, L. Durães, Progress in silica aerogel-containing materials for buildings' thermal insulation, *Constr. Build. Mater.* 286 (2021) (Article 122815).

[14] A. Lakatos, Z. Kovács, Comparison of thermal insulation performance of vacuum insulation panels with EPS protection layers measured with different methods, *Energy Build.* 236 (2021) 110771.

[15] Weitao Liang, Xiaobo Di, Shukui Zheng, Wu Leyu, Jianjun Zhang, A study on thermal bridge effect of vacuum insulation panels (VIPs), *J. Build. Eng.* 71 (2023) 106492.

[16] Jinfeng Wang, Xingxing Ma, Yuyao Sun, Jing Xie, Thermal performance and sustainability assessment of refrigerated container with vacuum insulation panel envelope layer at different design forms, *Thermal Sci. Eng. Prog.* 42 (2023) 101928.

[17] N. Simões, M. Gonçalves, C. Serra, S. Resalati, Can vacuum insulation panels be cost-effective when applied in building façades? *Build. Environ.* 107602 (2021).

[18] M.A. Mujebeu, N. Ashraf, A.H. Alsuwayigh, Effect of nano vacuum insulation panel and nanogel glazing on the energy performance of office building, *Appl. Energy* 173 (2016) 141–151.

[19] G. Eleftheriadis, M.M. Hamdy, The impact of insulation and HVAC degradation on overall building energy performance: a case study, *Buildings* 8 (2) (2018) 1–11.

[20] Maatouk Khoukhi, Shaimaa Abdelbaqi, Ahmed Hassan, Abeer Darsaleh, Impact of dynamic thermal conductivity change of EPS insulation on temperature variation through a wall assembly, *Case Stud. Thermal Eng.* 25 (2021) 100917.

[21] L. Aditya, T.M.I. Mahlia, B. Rismanchi, M.H. Hasan, H.S.C. Metselaar, Muraza, O. H.B. Aditya, A review on insulation materials for energy conservation in buildings, *Renew. Sust. Energy. Rev.* 73 (2017) 1352–1365.

[22] R. Coquard, D. Baillis, Thermal conductivity of Kelvin cell cellulosic aerogels: analytical and Monte Carlo approaches, *J. Mater. Sci.* 52 (19) (2017) 11135–11145.

[23] R. Galliano, K.G. Wakili, Th. Stahl, B. Binder, B. Daniotti, Performance evaluation of aerogel-based and perlite-based prototyped insulations for internal thermal retrofitting: HMT model validation by monitoring at demo scale, *Energy Build.* 126 (2016) 275–286.

[24] U. Berardi, The development of a monolithic aerogel glazed window for an energy retrofitting project, *Appl. Energy* 154 (2015) 603–615.

[25] U. Berardi, Aerogel-enhanced systems for building energy retrofits: insights from a case study, *Energy Build.* 159 (2018) 370–381.

[26] Xiaojian Wang, Gu Wenbo, Lu Hao, Effects of three-dimensional pore structure on effective thermal conductivities of thermal insulation materials, *Int. Commun. Heat Mass Transf.* 139 (2022) 106523.

[27] B.P. Jelle, Traditional, state-of-the-art and future thermal building insulation materials and solutions – properties, requirements and possibilities, *Energy Build.* 43 (2011) 2549–2563.

[28] B.P. Jelle, Accelerated climate ageing of building materials, components and structures in the laboratory, *J. Mater. Sci.* 47 (2012) 6475–6496.

[29] M.M. Koebel, A. Rigacci, P. Achard, Aerogels for superinsulation: A synoptic view, in: M.A. Aegerter, M. Prassas, M.M. Koebel (Eds.), *Aerogels Handbook — Advances in Sol-Gel Derived Materials and Technologies*, Springer, New York, Dordrecht, Heidelberg, 2011, pp. 607–633.

[30] M. Koebel, A. Rigacci, P. Achard, Aerogel-based thermal superinsulation: an overview, *J. Sol-Gel Sci. Technol.* 63 (3) (2012) 315–339.

[31] E. Cuce, P.M. Cuce, C.J. Wood, S.B. Riffat, Toward aerogel based thermal super insulation in buildings: a comprehensive review, *Renew. Sust. Energy. Rev.* 34 (2014) 273–299.

[32] EBC-Annex-65-Report-subtask-I-SoA-2020-01-03-v01.pdf (viba-international.org) (accessed on 22/12/2023).

[33] E. Cuce, P.M. Cuce, C.J. Wood, S.B. Riffat, Optimizing insulation thickness and analysing environmental impacts of aerogel-based thermal superinsulation in buildings, *Energy Build.* 77 (2014) 28–39.

[34] E. Cuce, P.M. Cuce, The impact of internal aerogel retrofitting on the thermal bridges of residential buildings: an experimental and statistical research, *Energy Build.* 116 (2016) 449–454.

[35] E. Cuce, et al., Experimental performance assessment of a novel insulation plaster as an energy-efficient retrofit solution for external walls: an essential building material towards low/zero carbon buildings, *Case Stud. Therm. Eng.* 49 (2023) 103350.

[36] E. Cuce, P.M. Cuce, E. Alvrur, Internal or external thermal superinsulation towards low/zero carbon buildings? A critical report, *Gazi Mühendislik Bilimleri Dergisi* 9 (3) (2024) 435–442.

[37] J. Fricke, H. Schwab, U. Heinemann, Vacuum insulation panels - exciting thermal properties and most challenging applications, *Int. J. Thermophys.* 27 (4) (2006) 1123–1139.

[38] S.E. Kalnas, B.P. Jelle, Vacuum insulation panel products: a state-of-the-art review and future research pathways, *Appl. Energy* 116 (2014) 355–375.

[39] U. Heinemann, Influence of water on the total heat transfer in 'evacuated' insulations, *Int. J. Thermophys.* 29 (2) (2008) 735–749.

[40] H. Simmler, S. Brunner, Vacuum insulation panels for building applications basic properties, ageing mechanisms and service life, *Energy Build.* 37 (11) (2005) 1122–1131.

[41] Martín-Garín Alexander, Rodríguez-Vidal Iñigo, Otaegi Jorge, Rico-Martínez José Miguel, Millán-García José Antonio, Senderos Laka María, Lucchi Elena, Hygrothermal performance analysis of building components and materials. A tool for energy refurbishments assessments, in: D. Bienvenido-Huertas, J. Durán-

- Álvarez (Eds.), Building Engineering Facing the Challenges of the 21st Century. Lecture Notes in Civil Engineering vol. 345, Springer, Singapore, 2023, https://doi.org/10.1007/978-981-99-2714-2_23.
- [42] P. Johansson, B. Adl-Zarrabi, A. Berge, Evaluation of long-term performance of VIPs, *Energy Procedia* 78 (2015) 388–393.
- [43] Á. Lakatos, M. Csontos, A. Csik, Investigation of both thermal parameters and applications of closed-cell plastic thermal insulation foams with building energetic aspects, *J. Therm. Anal. Calorim.* (2023) 1–26, <https://doi.org/10.1007/s10973-023-12789-8>. "Accepted by Publisher".
- [44] Á. Lakatos, Investigation of the moisture induced degradation of the thermal properties of aerogel blankets: measurements, calculations, simulations, *Energ. Build.* 139 (2017) 506–516.
- [45] A. Lakatos, Thermal insulation capability of nanostructured insulations and their combination as hybrid insulation systems, *Case Stud. Thermal Eng.* 41 (2023) 102630.
- [46] A. Nowoświat, P. Krause, A. Miros, Properties of expanded graphite polystyrene damaged by the impact of solar radiation, *J. Build. Eng.* 34 (2021) 101920.
- [47] Á. Lakatos, A. Csik, Multiscale thermal investigations of graphite doped polystyrene thermal insulation, *Polymers*. 14 (8) (2022) 1606.
- [48] Xiaoyu Yan, Ankang Kan, Zhaofeng Chen, Yulin Hei, Huanhuan Chen, Wu Weihui, A promising approach of caved vacuum insulation panel and investigation on its thermal bridge effect, *Int. Commun. Heat Mass Transf.* 148 (2023) 107086.
- [49] Kovács, Z.; Szanyi, S.; Budai, I.; Lakatos, Á., Laboratory tests of high-performance thermal insulations, In: Jain, Lakshmi C.; Capozzoli, Alfonso; Howlett, Robert J.; Littlewood, John (szerk.) *Sustainability in Energy and Buildings*, Singapore, Singapur: Springer Singapore (2020) pp. 73-82. Paper: Chapter 7, 10p.
- [50] Jiali Hu, Ying Qian, Tongjuan Liu, Tingxuan Wu, Guangyu Zhang, Wei Zhang, Preparation of needled nonwoven enhanced silica aerogel for thermal insulation, *Case Stud. Thermal Eng.* 45 (2023) 103025 (ISSN 2214-157X).
- [51] R.H. Nosrati, U. Berardi, Hygrothermal characteristics of aerogel-enhanced insulating materials under different humidity and temperature conditions, *Energ. Build.* 158 (2018) 698–711.
- [52] L.u. Jiayi, A. Kan, W. Zhu, Y. Yuan, Numerical investigation on effective thermal conductivity of fibrous porous medium under vacuum using Lattice-Boltzmann method, *Int. J. Therm. Sci.* 160 (2021). Article 106682.
- [53] J. Andersons, J. Modniks, M. Kirpluks, Modelling the effect of morphology on thermal aging of low-density closed-cell PU foams, *Int. Commun. Heat Mass Transf.* 139 (2022) 106432.
- [54] Jinpeng Feng, Meng Liu, Shaojian Ma, Jinlin Yang, Wei Mo, Su Xiujian, Micro-nano scale heat transfer mechanisms for fumed silica based thermal insulating composite, *Int. Commun. Heat Mass Transf.* 110 (2020) 104392.
- [55] I. Nardi, E. Lucchi, In situ thermal transmittance assessment of the building envelope: practical advice and outlooks for standard and innovative procedures, *Energies* 16 (8) (2023) 3319, <https://doi.org/10.3390/en16083319>.
- [56] M. Andreotti, et al., Design and construction of a new metering hot box for the hygrothermal measurement in dynamic condition of historic masonries, *Energies* 13 (11) (2020) 29–50, <https://doi.org/10.3390/en13112950>.
- [57] E. Lucchi, et al., Development of a compatible, low cost and high accurate conservation remote sensing technology for the hygrothermal assessment of historic walls, *Electronics* 8 (2019), <https://doi.org/10.3390/electronics8060643>.
- [58] E. Lucchi, R. Roberti, A. Troi, Definition of an experimental procedure with the hot box method for the thermal performance evaluation of inhomogeneous walls, *Energ. Build.* 179 (2018) 99–111, <https://doi.org/10.1016/j.enbuild.2018.08.049>.
- [59] H. Zhang, Y.X. Ma, X. Wang, G.H. Tang, Numerical study of the influence of thermal radiation on measuring semi-transparent thermal insulation material with hot wire method, *Int. Commun. Heat Mass Transf.* 121 (2021) 105120.
- [60] ISO 8301, Thermal insulation - Determination of steady-state thermal resistance and related properties - Guarded hot plate apparatus, 1991.
- [61] EN 1946–2, Thermal performance of building products and components - Specific criteria for the assessment of laboratories measuring heat transfer properties - Part 2: Measurements by guarded hot plate method, 2001.
- [62] EN ISO 12667, Thermal performance of building materials and products. Determination of thermal resistance using guarded hot plate and heat flow meter methods, in: *Products of High and Medium Thermal Resistance*, 2001.
- [63] EN 12664, Thermal performance of building materials and products -Determination of thermal resistance by means of guarded hot plate and heat flow meter methods - Dry and moist products of medium and low thermal resistance, 2002.
- [64] ASTM 177, Standard Test Method for Steady-State Heat Flux Measurements and Thermal Transmission Properties by Means of the Guarded-Hot-Plate Apparatus, 2010.
- [65] ASTM 1043, Standard Practice for Guarded-Hot-Plate Design Using Circular Line-Heat Sources, 2019.
- [66] ASTM C1044-16:2020. Standard Practice for Using a Guarded-Hot-Plate Apparatus or Thin-Heater Apparatus in the Single-Sided Mode.
- [67] ISO 8302, Thermal insulation - Determination of steady-State Thermal Resistance and Related Properties - Heat Flow Meter Apparatus, 1991.
- [68] EN 1946–3, Thermal performance of building products and components - Specific criteria for the assessment of laboratories measuring heat transfer properties - Part 3: Measurements by heat flow meter method, 1999.
- [69] ASTM C 518, Standard Test Method for Steady-State Thermal Transmission Properties by Means of the Heat Flow Meter Apparatus, 2010.
- [70] ASTM C1363-19. Standard Test Method for Thermal Performance of Building Materials and Envelope Assemblies by Means of a Hot Box Apparatus.
- [71] ISO 8894-1, Refractory materials, in: *Determination of Thermal Conductivity. Part 1: Hot-Wire Methods (Cross-array and Resistance Thermometer)*, 2010.
- [72] EN 993–15, Methods of Test for Dense Shaped Refractory Products - Part 15: Determination of Thermal Conductivity by the Hotwire (parallel) Method, 2005.
- [73] ASTM C1113, Standard Test Method for Thermal Conductivity of Refractories by Hot Wire, Platinum Resistance Thermometer Technique, 2013.
- [74] ASTM E 1461, Standard Test Method for Thermal Diffusivity by the Flash Method, 2013.
- [75] EN ISO 8990: Thermal Insulation, Determination of Steady-State Thermal Transmission Properties Calibrated and Guarded hot Box.
- [76] C. Jang, H. Jung, J. Lee, T.-H. Song, Radiative heat transfer analysis in pure scattering layers to be used in vacuum insulation panels, *Appl. Energy* 112: 703–709.
- [77] J. Yang, S. Li, H. Jiang, C. Su, Y. Shao, Y. Gao, J. Li, Preparation of recycled graphite/expanded polystyrene by a facile solvent dissolution method, *J. Mater. Sci.* 54 (2019) 1197–1204.
- [78] E. Lucchi, et al., Thermal performance evaluation and comfort assessment of advanced aerogel as blown-in insulation for historic buildings, *Build. Environ.* 122 (2018) 258–268.
- [79] J. Pan, F. Chen, D.E. Cabrera, Z. Min, S. Ruan, M. Wu, D. Zhang, J.M. Castro, J. L. Lee, Carbon particulate and controlled-hydrolysis assisted extrusion foaming of semicrystalline polyethylene terephthalate for the enhanced thermal insulation property, *J. Cell. Plast.* 57 (2021) 695–716.
- [80] J. Pan, D. Zhang, M. Wu, S. Ruan, J.M. Castro, J.L. Lee, F. Chen, Impacts of carbonaceous particulates on extrudate semicrystalline polyethylene terephthalate foams: nonisothermal crystallization, rheology, and infrared attenuation studies, *Ind. Eng. Chem. Res.* 59 (2020) 15586–15597.